Embedded Optimization for Space Rider Re-entry Module Parafoil GNC

J. Ramírez [(1)], L. Hewing [(1)], F. Cacciatore [(1)], J. Cardín [(1)], M. Lucrezia [(1)], V. Preda [(2)]

[(1)] SENER Aeroespace, C/Severo Ochoa, 4 – 28760 Tres Cantos, Madrid, Spain,
jesus.ramirez@aeroespacial.sener
[(2)] ESA/ESTEC, Keplerlaan 1, PO Box 299, 2200 AG Noordwijk, The Netherlands,
valentin.preda@esa.int

ABSTRACT

This paper addresses the very final part of the Space Rider Re-entry Module landing under parafoil, known as the flare, for which we demonstrate the suitability of a Model Predictive Control (MPC) scheme to control the parafoil in closed-loop to minimize the impact velocity. The optimization problem is formulated as a convex quadratic program which is subsequently solved by a tailored interior point solver developed in-house at SENER Aeroespacial. We give a sketch of the entire engineering pipeline, including a data-driven identification of low complexity linear system models capturing the relevant dynamics for the flare execution. Furthermore, we outline several design characteristics important for achieving the desired results, such as robustifying the formulation against uncertainties using a constraint-tightening scheme. The developed algorithms are supported by theoretical convergence guarantees and extensively tested on representative hardware empirically demonstrating their real-time reliability. Results show major improvements in the landing performance under realistic wind conditions and system uncertainties when compared with open-loop lookup tables. As an outcome of the success of the implementation, the MPC Flare and the optimization core end-to-end developed and tailored by SENER Aeroespacial will be proven in real flight in within the Space Rider Scale Down Flight Tests in 2023.

1 INTRODUCTION

Space Rider (SR) is a European Space Agency (ESA) program with the purpose of developing an affordable and sustainable reusable space transportation system [1]. The SR vehicle is composed of two modules: the AVUM Orbital Module (AOM) and the Re-Entry Module (RM). Together, they will serve as platform for in-orbit operation, experimentation, and demonstration of applications, and will enable the access to and return from space in a safe and efficient way. For Space Rider, SENER Aeroespacial is the Design Authority of the RM Guidance, Navigation, and Control (GNC), under contract with TAS-I, prime contractor for the RM development. Pushing forward reusability and landing accuracy, the RM uses a guided parafoil during the descent and landing phase for a pinpoint touchdown without additional propellant use. This phase starts approximately at 5.5 km above ground level, after having completed the rest of the re-entry mission phases: orbital coasting up to the entry interface point, hypersonic entry flight, transonic pass, and descent under parachute. The Parafoil Guidance, Navigation, and Control (PGNC) drives the system to land within 150 meters from the target compensating wind drift and dispersions accumulated during the previous phases, all the while ensuring a soft touch down.

Figure 1. SR RM parafoil guidance phases

The PGNC is divided in various modes attending to the different parts of the parafoil phase depicted in Fig. 1. This paper addresses the very final part of the landing: a window of a few seconds in which the vehicle needs to reduce its vertical velocity below a threshold to meet the landing gear impact requirements. The impact velocity requirements are very stringent in order to guarantee the integrity of the structure and units to ensure reuse: <15 m/s in horizontal velocity, <1 m/s in lateral velocity, and <3.5 m/s in vertical velocity. Especially the last requirement poses a challenge to the PGNC, as the SR maximum vertical touchdown velocity is equivalent to a free fall from just 62 cm. To meet the requirement, a manoeuvre known as the flare is used to reduce the vertical velocity, typically consisting of a simultaneous full deflection of the parafoil winches triggered at the correct altitude to induce a momentary reduction in the vertical vehicle velocity [3].

This manoeuvre is commonly executed in open-loop based on lookup tables (LUT) to select the triggering altitude based on mass and the current symmetric stroke. While this approach may be sufficient under favourable weather conditions, severe winds combined with large system uncertainties can lead to impacts at speeds greatly exceeding the allowed maximums. To reduce this risk and improve the PGNC performance, a Model Predictive Control (MPC) is implemented controlling the system in closed-loop during the flare.

MPC is an advanced control technique based on onboard optimization which has shown enormous success and is generating great interest in the aerospace sector [4]. However, even though proofs of its potential in this sector have been demonstrated, e.g., in the SpaceX reusable boosters [5], its implementation in space graded HW is often hindered by its computational complexity. The MPC for the SR presented in this paper is based on a linear system model tailored to the transient flare dynamics to be optimized. This allows to formulate the optimization problem as a convex quadratic program that can be reliably solved in real-time.

In order to meet computation performance requirements and keep full control of the GNC software, the problem is solved by an Interior Point Method (IPM) algorithm developed in-house at SENER Aerospace and tailored to exploit the specific problem structure and sparsity. The computational and algorithmic complexity is further reduced making use of a condensed formulation and a Move Blocking (MB) scheme [6], reducing the number of optimization variables. The MPC is then applied in a shrinking horizon fashion to control the flare in closed-loop to minimize the impact velocity, recomputing the optimal parafoil strokes at a frequency of 2.5Hz. The trajectory predictions provided by MPC are actively used to refine the time-to-touchdown estimates, which are integral for defining the objective function of the MPC optimization, namely exploiting the transient system dynamics to minimize vertical velocity at the estimated touchdown.

The MPC improves thus the open-loop approach in three major aspects: (1) time predictions are actively corrected so that minimum in vertical velocity is achieved at the actual instance of impact; (2) the exact system state and its transient dynamics are fully exploited leading to higher performance in terms over minimum vertical velocity achieved; and (3) robustness against uncertainties and wind is improved due to closed-loop feedback. In line with the point (3), mitigation strategies are implemented to further improve the MPC actuation under system uncertainties and in particular wind. These strategies include robustification of the scheme with constraint tightening [7], addition of a wind correction heuristics to improve the time predictions, and optimization adaptation to explicitly account for time prediction uncertainties.

The success of the implementation, both in results and computation efficiency, has led to accept the MPC as part of the Scale Down Flight Tests (SDFT) campaign to be performed in 2023 to validate the SR PGNC [2]. The test will be used not only to demonstrate the real-time feasibility and performance, but also to demonstrate the possibility of further improving the dynamic model by fitting experimental data in the system identification. The implementation of the MPC as part of the baseline PGNC of the SR is envisioned after the SDFT demonstrations.

This paper is organized as follows. Section 2 describes the system behaviour during the flare and the linearization based on System Identification performed. Section 3 continues presenting the MPC for the flare, including the formulation and implementation details. Section 4 then outlines the SENER Optimization Toolbox (SOTB), used for solving the optimization problem. Finally, Section 5 show performance results and comparisons with open-loop approaches, and Section 6 closes with a summary and conclusions.

2 FLARE DYNAMICS

The parafoil phase of the SR RM is controlled only by means of the two parafoil winches' release and pull. The average between the right (l_R) and left (l_L) winches length is called the symmetric stroke (X_s), while half of the difference is called the asymmetric stroke (X_a), as depicted in Eq. 1.

$$X_s = \frac{l_R + l_L}{2};\ X_a = \frac{l_R - l_L}{2}; \tag{1}$$

Symmetric and asymmetric stroke can be then mapped in steady state conditions to flight path angle and heading rate [8], i.e., to control horizontally al laterally respectively the trajectory. These two variables constitute the pillars of the PGNC up to the flare. For the very last part of the landing, however, in which interest lies on controlling the vertical velocity, the control variable becomes only the symmetric stroke. This means that the spacecraft is controlled neither horizontally nor laterally during the last meters of the re-entry mission, in the previous PGNC modes have will already have correctly pointed the SR RM towards the landing point and with front wind at touchdown [8]. The flare manoeuvre is characterized by the symmetric pull/release of the winches which induces a transient dynamic response in the system that allows to reach vertical velocities outside the range of steady state conditions. In Fig 2, the relevant system variables for the flare are represented for a typical symmetric stroke profile commanded by the MPC (in ideal conditions) from trim conditions. The system response under such actuation, even if non-linear, resembles damped spring dynamics for each of the state variables with the symmetric stroke as input, where:

- Vertical velocity oscillates achieving a maximum value followed by a minimum. In the steady state, the value does not greatly differ from the initial condition.
- Horizontal velocity oscillates in a similar way to the vertical velocity. However, the minimum location is delayed in time with respect to instant corresponding to vertical velocity minimum. Aside from that, the steady state differs from the initial condition.
- Pitch behaves like horizontal velocity.

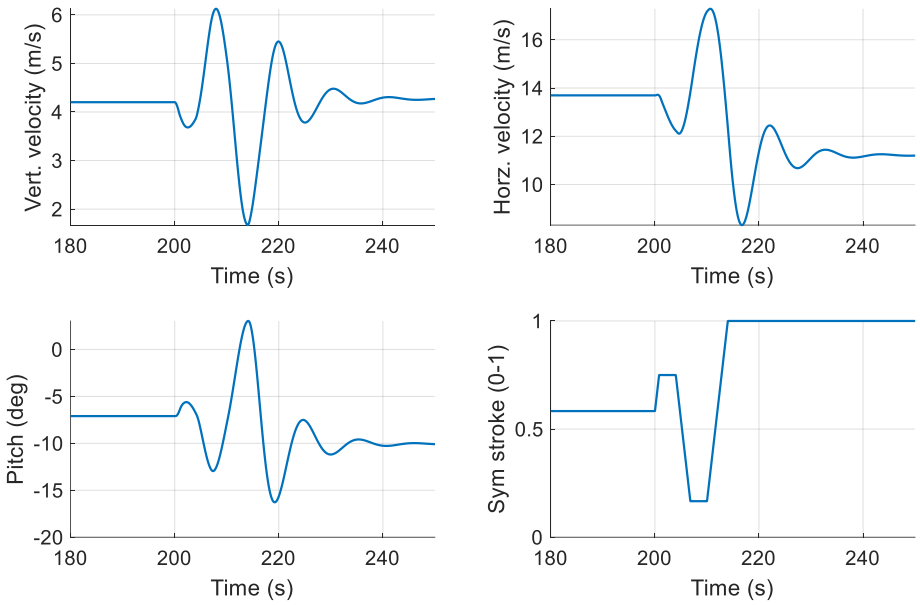

Figure 2. System behaviour during flare, from simulation in ideal conditions

2.1 System Identification

While the parafoil dynamics are generally non-linear, the previous discussion highlights that it may be possible to find a reasonably simple and highly representative linear description of the fare dynamics. Since the MPC is used to minimize the vertical velocity, and in order to reduce both computational complexity and complexity of the system identification, a single-input single-output (SISO) is developed mapping the symmetric stroke (input) and the vertical velocity (output). As outlined previously, this linear model choice will lead to a low complexity, convex optimization problem to be solved as part of the MPC.

Given the observed typical damped oscillatory behaviour a simple second order linear system is to be fitted to recorded nonlinear simulations. A transfer function is obtained from a system identification procedure based on regression model fitting method fed with hundreds of simulations of the SR RM parafoil phase. The simulations come from Monte Carlo (MC) campaigns in which initial conditions are varied and aerodynamic and mass uncertainties expected on the real mission included, aiming to find a linear model that is “robustly” applicable. The wind is not added in these campaigns since its strong decay with altitude in the last meters induce non-linear wind-profile-dependent effects that hinder the fitting of a single linear model. Instead, wind effects are considered by the MPC by other means rather than explicitly considering it on the dynamics. To generate representative excitations for fitting the system response during the flare, simulations are first carried out using the PGNC based on LUT, and in a second iteration of the system identification is later performed with simulations using a preliminary MPC improving the representativeness for the final implementation. Note that more iterations of the process can be done to further refine the linearized dynamic model.

Summarizing, the System Identification used for linearizing the flare dynamics consist of:

1. Simulations are carried out with the open loop LUT flare, with:
    a. Mass perturbation.
    b. Aerodynamic database perturbation.
    c. No error on sensors.
    d. No wind.
2. Vertical velocity and symmetric stroke data during the flare manoeuvre are recorded.
3. A regression model fitting method is applied to identify a second-order transfer function from symmetric stroke to vertical velocity.
4. The model is discretized and used in MPC.
5. Simulations are repeated with the MPC, and process from point 2 repeated to refine the linearization around the MPC manoeuvres.

The system identification can be repeated with experimental data to refine the model. This operation is expected to be performed during operation phases of the SR and will be done as part of the SDFT campaign.

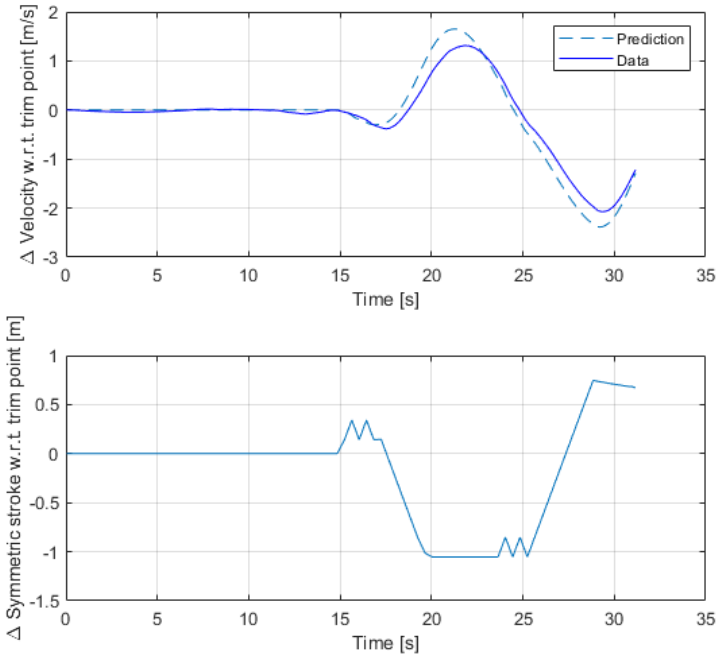

Figure 3. Comparison between linearized model and realistic simulation with non-linear dynamics

2.2 Discretized system model

The transfer function obtained through the system identification is discretized with a Zero Order Hold (ZOH) scheme to obtain a linear system canonical form in which one of the variables is the output (vertical velocity with respect to the trim point). The resulting dynamics can be expressed in state-space form as

$$\begin{bmatrix} v_{i+1} \\ w_{i+1} \end{bmatrix} = \bar{A} \begin{bmatrix} v_i \\ w_i \end{bmatrix} + \bar{B} x_i. \tag{2}$$

Here, the variables v and x are the vertical velocity and symmetric stroke with respect to the trim point, respectively, and w an auxiliar variable resulting from the 2nd order transfer function. In order to include actuator rate limitations, the model is extended in an input integration fashion, resulting in:

$$\begin{bmatrix} v_{i+1} \\ w_{i+1} \\ x_{i+1} \end{bmatrix} = \begin{bmatrix} \bar{A} & \bar{B} \\ 0 & 1 \end{bmatrix} \begin{bmatrix} v_i \\ w_i \\ x_i \end{bmatrix} + \begin{bmatrix} 0 \\ 0 \\ \Delta T \end{bmatrix} u_i = A \begin{bmatrix} v_i \\ w_i \\ x_i \end{bmatrix} + B u_i; \tag{3}$$

with u the symmetric stroke rate and ΔT the discretization step. The initial conditions for the MPC can be directly obtained from the PGNC navigation data except for the auxiliar variable $\overline{w_0}$, which can be obtained from the previous step with:

$$\overline{w_0} = A_{21} v_{-1} + A_{23} x_{-1}. \tag{4}$$

Note that the control canonical form of the system is obtained so that $A_{22} = 0$, and that data from previous step is already available in the first call to the MPC.

3 MODEL PREDICTIVE CONTROL FOR FLARE

The flare has its own PGNC mode, in which the MPC is implemented to control the winches in closed-loop to minimise the vertical landing velocity. In the PGNC, the guidance block computes a flight path angle and heading rate to be followed, and then the control tracks it at a higher frequency. This differentiation in frequencies is maintained in the flare mode, but the interfaces change. The MPC works at the guidance frequency, and the control function and interface are modified to receive and execute a symmetric stroke rate and asymmetric stroke. The asymmetric stroke is commanded to zero through the entire manoeuvre, while the MPC commands a symmetric stroke rate to be maintained until next the next guidance call. This scheme, sketched in Fig.4, is kept for:

- Reducing the number of PGNC modifications for implementing the MPC.
- Maintaining SW and avionics working frequencies.
- The PGNC guidance frequency allows to work with a suitable discretization scheme.
- Some functionalities of the control are still required to manage and translate asymmetric stroke and symmetric stroke rate into actuator commands.
- MPC command is followed as planned (ZOH in stroke rate).

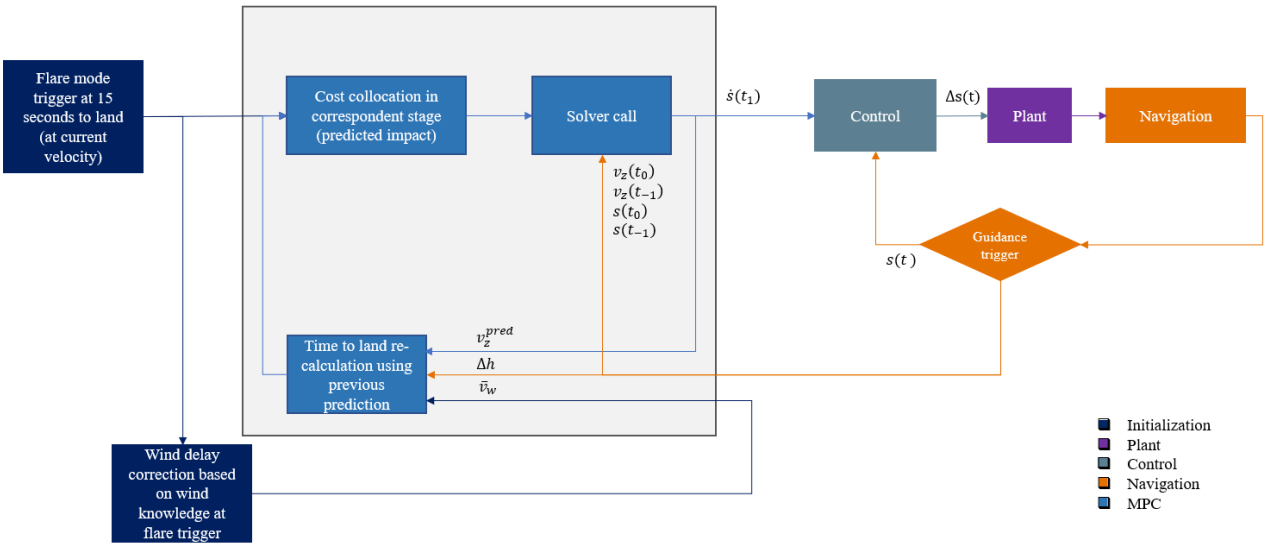

Figure 4. PGNC flare mode architecture with MPC

The MPC receives from the navigation the vertical velocity and symmetric stroke at the current instant and at the previous guidance step to compute the complete initial conditions, as shown in Eq. 4. It also receives a time prediction based on the previous MPC solution to minimize the velocity corresponding to the landing instant. With these inputs, the optimisation problem is solved, and a symmetric stroke rate commanded to the control.

The following sections present the Numerical Optimal Control Problem (NOCP) formulation for the MPC, a Move Blocking (MB) scheme implemented to reduce the size of the problem, and the time prediction algorithm that accounts for wind effects.

3.1 Numerical Optimal Control Problem Formulation

The NOCP of the MPC for the flare control is formulated as a quadratic program with polytopic constraints in which the vertical velocity is minimised at the predicted landing time. The identified model for linearizing the dynamics is used and the problem formulation kept convex:

$$\min_{v_i, w_i, x_i, u_i} \quad c_N v_N + \sum_{i=0}^{N-1} \frac{1}{2} u_i^T R u_i + c_i v_i \,; \tag{5}$$

$$s.t. \quad [v_{i+1}, w_{i+1}, x_{i+1}]^T = A[v_i, w_i, x_i]^T + B u_i; \quad i = 0,1,\dots,N-1; \tag{6}$$

$$u_{i_{min}} \leq u_i \leq u_{i_{max}}; \quad i = 0,1,\dots,N-1; \tag{7}$$

$$x_{min} \leq x_i \leq x_{max}; \quad i = 0,1,\dots,N-1; \tag{8}$$

$$[v_0, w_0, x_0]^T = [\overline{v_0}, \overline{w_0}, \overline{x_0}]^T \tag{9}$$

where v, w, x and u are the optimisation variables, corresponding to system states and input with transition matrices A and B as in Eq. 3; R and c are the quadratic and linear cost; u_{min}, u_{max}, x_{min} and x_{max} are the stroke rate and symmetric stroke limits, respectively; and $[\overline{v_0}, \overline{w_0}, \overline{x_0}]^T$ are the initial conditions, i.e., the system state at the MPC call. The subindex i marks the stage in the horizon of N collocation points.

To match the velocity stage minimized with the predicted time to land, the linear cost c is adapted online. The cost vector is built from the predicted time and uncertainty as showed in Fig. 5, where the blue cost represents the resultant cost without time uncertainty included, i.e., closest stage to the landing point within the prediction horizon. The quadratic cost on the input R is maintained for all the stages, working as a regulator term. With this approach, the MPC behaves as a shrinking horizon scheme, but for implementation purposes the actual horizon length remains constant.

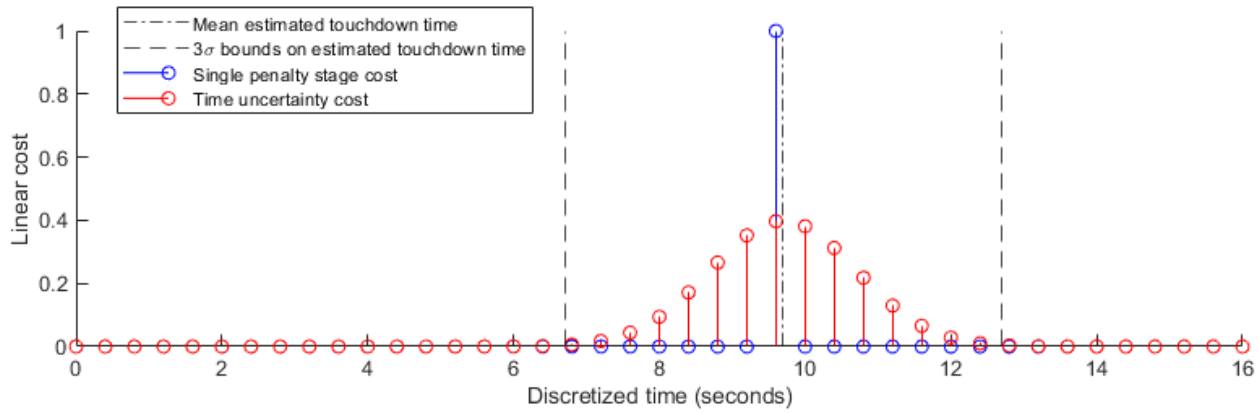

Figure 5. Linear cost adaptation with time prediction

An important feature of the MPC is that the input is constrained with the real actuator limitation: the winch rate. In this way, the MPC output can be tracked by the control, so predictions better match reality. The actual constraint is constant and time invariant. However, the NOCP formulation is robustified with a constraint tightening varying in the horizon as showed in Fig. 6. With this implementation, a robust MPC is obtained in which actuation margin is saved for the future at the prediction level, although the full envelope is exploited in closed-loop. This scheme is useful for counteracting system uncertainties and specially the wind-drop effects.

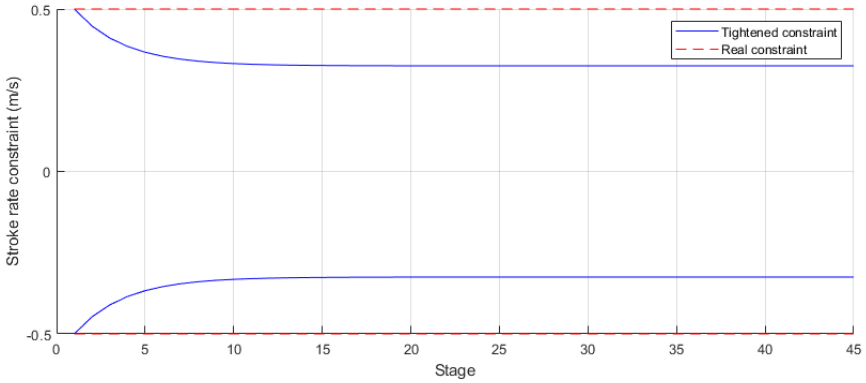

Figure 6. Control tightening constraint

3.2 Move Blocking scheme

To further reduce computational burden, a MB scheme is implemented [6]. The strategy allows to arbitrary reduce the number of variables by forcing some inputs to be equal to the one in its predecessor stage, i.e., by freezing some inputs variation in the prediction horizon. The resultant problem is conceptually equal to work simultaneously with ZOH with different discretization steps, as sketched in Fig 7.

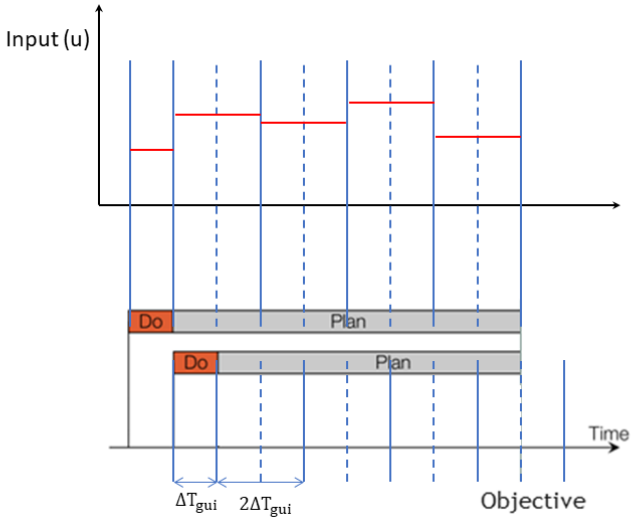

Figure 7. Move Blocking scheme

This MB policy implemented has not noticeable effects over the optimum of the NOCP. Issues related with constraint violation in states or inputs for the frozen steps does not appear in the specific problem aside from the constraint tightening, which is an artificial construction and does not affect the feasibility of the original problem. On the other hand, there is no decrease of accuracy regarding the minimization of the stage correspondent to the impact since original discretization is maintained in the cost function. Finally, the system exploitation is neither affected since solutions without MB typically maintain the same input either at zero or saturated for a few stages, and for the very end of the manoeuvre saturation of the symmetric stroke is pursued.

3.3 Time prediction with wind correction

Minimising the vertical velocity at the touchdown constitutes a nonlinear problem that couples altitude and velocity. To avoid the nonlinearity, vertical velocity is minimised at a previously predicted impact time. This means that, if the integral of the vertical velocity profile differs from the used to compute the prediction time, vertical velocity is minimized at the wrong stage. To deal with this issue, prediction time is updated between MPC calls by integrating the latest prediction with the current altitude. Furthermore, a heuristic-based correction is added to the predicted time based on the wind drop from flare triggering to landing aiming to capture part of the wind effects over the dynamics. This approach has shown quick convergence between prediction time before and after the MPC call, as shown in Fig. 8. Note that as the SR approaches the landing, errors in prediction time become smaller due to reduced model error propagation, lower wind change effects, and less influence of the robust scheme for which predictions vary between calls. The effects of the wind and the robust scheme are further discussed in the results section.

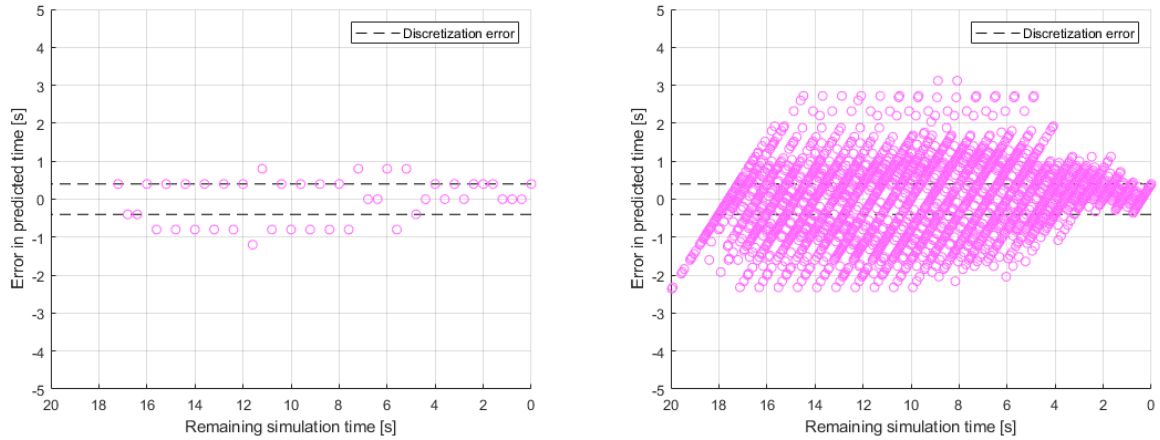

Figure 8. MPC prediction time error. Single case (left) and 1000 shots MC campaign (right)

4 SENER OPTIMIZATION TOOLBOX (SOTB)

The SENER Optimization Toolbox (SOTB) [9] is an autocodable MATLAB implementation of a toolbox for numerical optimal control which is independent of other MATLAB toolboxes or external software. It contains functions developed in-house for general numerical optimization with a specific focus on optimal control, including dedicated interior-point solvers tailored for exploiting typical MPC structures and Sequential Convex Programming (SCP) algorithms for non-linear problems. The current state of the development allows the research and quick prototyping of optimal control problems and is being tested in industrial applications. The following sections give a brief overview of the interior-point solver used in the SR MPC flare, as well as some results on performance tests carried out in representative hardware.

4.1 Linear Model Predictive Control solver (sotbLMPC)

The solver used in the SR MPC is a tailoring of the SOTB function sotbLMPC. This function is based on an interior-point method (IPM) tailored for the solution of Linear MPC schemes in condensed form. This tool solves problems of the form:

$$\min_{v_i, w_i, x_i, u_i} \quad \min_{U} \frac{1}{2} U^T H U + c^T U \tag{10}$$

$$s.t. \quad A_{ineq} U \leq b_{ineq} \tag{11}$$

where the problem is convex, i.e., $H \succcurlyeq 0$, and U is a vector including the input variables of a NOCP in all the stages of the prediction horizon. H, c, A_{ineq}, and b_{ineq} condense the structure of a NOCP like the one on Eq. 5-9 to remove the state variables from the optimization variables. This approach, known as single-shoot method or dense formulation, can benefit the computation performance of the solver depending on the specific optimization problem and implementation [10-12], and benefits indeed the SR MPC whose dynamics are stable. Note that the problem condensing is done offline once and used online in the SR PGNC as part of the loaded database.

The sotbLMPC solver is based on a primal-dual interior-point method [10-12] which aims to solve the first optimality condition of Eq. 10-11, that is the Karush-Kuhn-Tucker (KKT) conditions. Given suitable constraints qualification, these conditions are necessary and sufficient for optimality and can expressed as:

$$\begin{bmatrix} HU + c + A_{ineq}^T \mu \\ \mu_i s_i \\ A_{ineq} U - b_{ineq} + s \end{bmatrix} = \begin{bmatrix} 0 \\ 0 \\ 0 \end{bmatrix} \tag{12}$$

where μ is a Lagrange multiplier and $s > 0$ a vector of slack variables. The non-linear system is then solved in a similar fashion to the one of sotbQCQP described in [9]. Nonetheless, sotbLMPC exploits the system structure and symmetry to reduce number of operations. Furthermore, the solver implemented for the SR MPC is tailored to the specific problem so that structure and symmetries are further exploited, and sparsity considered. Note that the MPC works in a receding horizon fashion, so the size and structure does not change between calls.

4.2 Performance tests

The reduction of variables and problem structure exploitation achieved with the dedicated solver result in a highly efficient MPC that can be executed in real-time. To demonstrate the real-time feasibility of the developed algorithms, the MPC (including sotbLMPC) is autocoded and implemented in an Arduino Portenta H7 board, with a 32 bits ARM Cortex M7 core. Preliminary results show convergence in less than 10 iterations of the solver in all the tested cases, and a computation time in the representative HW below the 7.5 ms in single float precision. This execution time is compliant with the control frequency and the scheduler in charge of receiving sensor data, pre-processing, calling the PGNC & MPC algorithms, commanding the actuators and data logging. This demonstrates the feasibility of the real-time implementation of the MPC for the SDFT, in which the board used for testing will be implemented as the onboard computer. For the SR mission, the results indicate feasibility due to representativeness of the testing HW, yet the MPC algorithms shall be tested on the GR740 (Leon4) 32 bits processor for full validation.

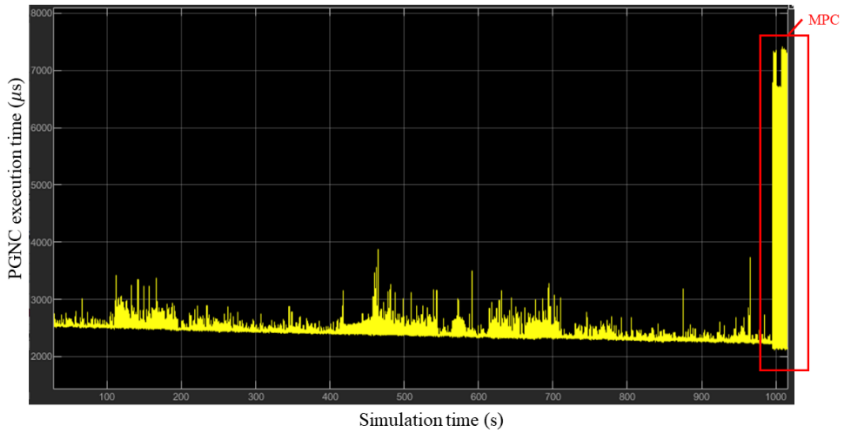

Figure 9. PGNC execution times through parafoil phase (time in μs)

5 RESULTS

In this section, the performance of the MPC for the SR flare is compared with the execution of the final manoeuvre based on open-loop LUT. Results are obtained with SENER's SR RM 6 DoF simulation environment used to develop and test the PGNC algorithms. The following perturbation and uncertainties are considered:

- Aerodynamic perturbations with respect to on-board database.
- Mass, inertia, and centre of gravity dispersions.
- Differential GPS (used for velocity) and radar altimeter (used for height) navigation errors.
- Wind profiles generated by Mesoscale simulations for Kourou landing site.
- Onboard wind tables errors.

This results section is focused on the achieved reductions on the vertical touchdown velocity, critical point for the use of open-loop LUT. Nonetheless, the use of the MPC has also shown an improvement in the horizontal velocity and no effects over the lateral velocity at landing, resulting in the overall accomplishment of the touchdown velocities requirements.

The Fig. 10 compares the vertical velocities achieved at landing (left plot) and profiles (mid and right plots) with the use of LUT and MPC in a situation without wind. Note that profiles are shown beyond landing time by maintaining maximum symmetric stroke to demonstrate that minimum in velocity is achieved at touchdown. The results show that the open-loop LUT manoeuvre is not sufficient for reducing the touchdown velocity below the requirement, while the MPC manages to reduce it down to 1.76 m/s average with a margin in the 99% percentile with a 90% confidence level of 0.8 m/s below the requirement. On the central plot it can also be seen that the minimum in velocity is achieved close to the landing point, with an offset of around one second. Note that the robust scheme introduces some variation between solution. This introduces a tendency of achieving the minimum in vertical velocity slightly before landing, which is beneficial for the horizontal velocity as shown in Fig. 2 and keeps margin for further reduction in some worst cases with wind.

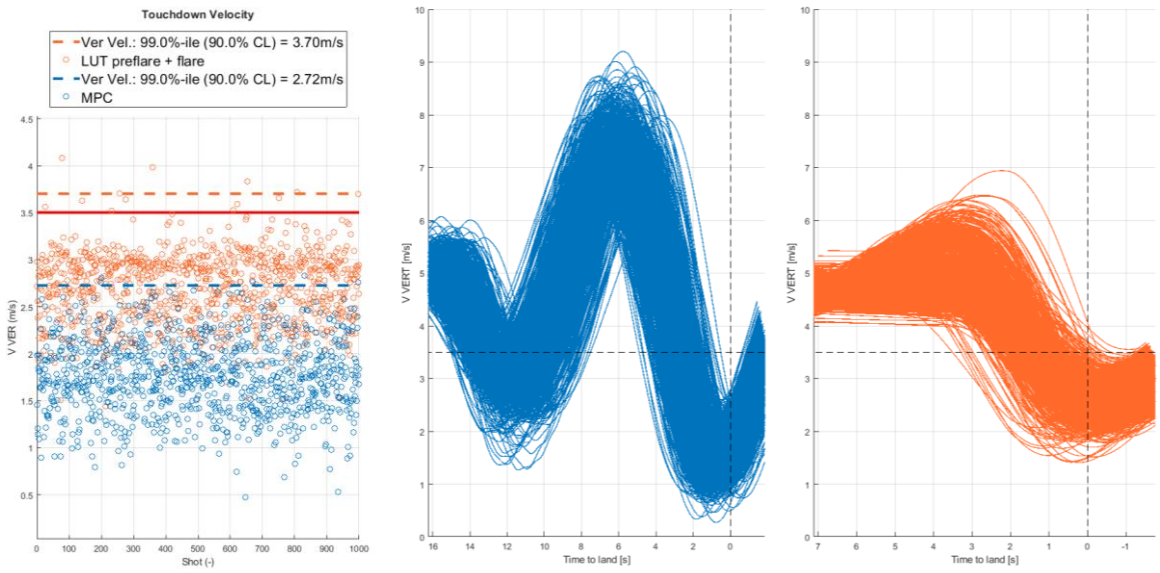

Figure 10. 1000 cases MC campaign without wind

The use of the open-loop LUT could be still considered as an option with some efforts on further tuning it if not by the effects of the wind. Indeed, the wind variation during the flare which induces non-predictable lift increases/decreases significantly degrades the performance with open-loop LUT. The Fig. 11 show the performance against the use of the MPC. While with the open-loop flare the requirement is exceeded in more than 1 m/s, with the use of the MPC the requirement is met in the 99% percentile with 90% confidence with almost 0.4 m/s of margin. The average landing velocity with MPC is increased to just 2.02 m/s with the presence of wind, and only two outliers exceed the requirements in the 1000 shots. These two cases have been correlated with non-common wind profiles that differs from the average wind behaviour from which correction heuristics are obtained. To deal with them, actuation winch speed has been agreed to be increased. With the extra actuation capabilities, the MPC manages to further reduce landing velocity and avoids any outlier. Finally, in the central plot it can be appreciated that thanks to the implementation decision taken, even if the minimum for the best cases is yet anticipated with respect landing instant, the minimum of the worst cases coincide with touchdown.

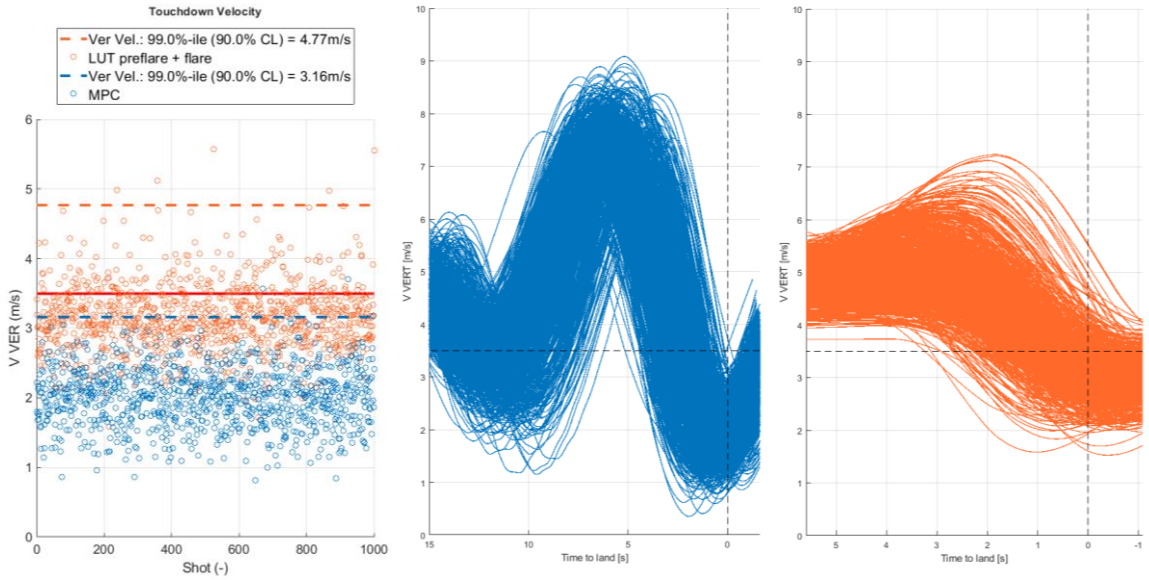

Figure 11. 1000 cases MC campaign with wind

6 CONCLUSIONS

An MPC for the closed-loop control of the SR RM during the final flare manoeuvre has been presented in this paper. The convex formulation of the NOCP together with the use of in-house developed optimization tools (SOTB) have demonstrated real-time performance in representative hardware. It was furthermore shown that the use of the MPC presents significant improvements over typical open-loop flare manoeuvres based on LUT. Results obtained in a realistic simulation environment demonstrate that the use of the MPC allows to reduce landing velocity below the 3.5 m/s requirement with a 0.4 m/s margin in the 99% percentile with 90% confidence level in the most demanding scenario, i.e., in the presence of aerodynamic database perturbations, mass uncertainties, navigation errors, and especially wind variation. The success of the MPC implementation has led the SR team to consider it part of the baseline PGNC of the RM. In the path towards the SR first flight, the MPC is to be tested with the rest of the PGNC in the SDFT campaigns to be run on 2023. The experiments will be used to further refine the dynamic models and will serve to validate and verify the MPC performance.

7 REFERENCES

[1] Cacciatore, F., et al. *The Design of the GNC of the Re-Entry Module of Space Rider*, EUCASS, Escuela Técnica Superior de Ingeniería Aeronáutica y del Espacio, Universidad Politécnica de Madrid, 2019. https://doi.org/10.13009/EUCASS2019-1016

[2] Cardín, J., et al, *Space Rider Re-Entry Module Scaled Down Flight Test Campaign*, ESA GNC-ICATT, 2023

[3] Figueroa, A., Cacciatore, F., and Haya Ramos, R., *Landing Guidance Strategy of Space Rider* Journal of Spacecraft and Rockets, 2021. 58. 1-12. 10.2514/1.A34957

[4] Eren, U., et al., *Model Predictive Control in Aerospace Systems: Current State and Opportunities*, Journal of Guidance, Control, and Dynamics, 2017. 40. 1541-1566. 10.2514/1.G002507

[5] Blackmore, L., *Autonomous precision landing of space rockets*, The Bridge, 46. 15-20, 2021

[6] Cagienard, R., et al., *Move blocking strategies in receding horizon control*, Journal of Process Control - J PROCESS CONTROL, 2007. 17. 10.1016/j.jprocont.2007.01.001

[7] Bemporad, A., Morari, M., *Robust model predictive control: A survey*. In: Garulli, A., Tesi, A. (eds) Robustness in identification and control. Lecture Notes in Control and Information Sciences, vol 245. Springer, London, 1999. https://doi.org/10.1007/BFb0109870

[8] Cardín, J., et al., *Space Rider Re-Entry Module GNC*, HiSST: 2nd International Conference on High-Speed Vehicle Science Technology, Bruges, Belgium, September 2022.

[9] Ramírez, J., Hewing, L., *Sequential Convex Programming for Optimal Line of Sight Steering in Agile Missions*, 9th European Conference for Aeronautics and Aerospace Sciences (EUCASS), 2022. https://doi.org/10.13009/EUCASS2022-7361

[10] Dehl, M., and Gros, S., *Manuscript of Numerical Optimal Control*, University of Freiburg, 2020.

[11] Nocedal, J., Wright, S.J., *Numerical Optimization*, Springer, New York, 2006. https://doi.org/10.1007/978-0-387-40065-5

[12] Jerez J. L., Kerrigan E. C., and Constantinides, G. A., *A condensed and sparse QP formulation for predictive control*, 2011 50th IEEE Conference on Decision and Control and European Control Conference, Orlando, FL, USA, 2011, pp. 5217-5222, doi: 10.1109/CDC.2011.6160293.